Distribution of non-ceruloplasmin-bound copper after i.v. ^{64}Cu injection studied with PET/CT in patients with Wilson disease

Authors

Ditte Emilie Munk, Mikkel Holm Vendelbo, Frederik Teicher Kirk, Karina Stubkjær Rewitz, Dirk Andreas Bender, Karina Højrup Vase, Ole Lajord Munk, Hendrik Vilstrup, Peter Ott, Thomas Damgaard Sandahl

Correspondence

dittmu@rm.dk (D.E. Munk).

Graphical abstract

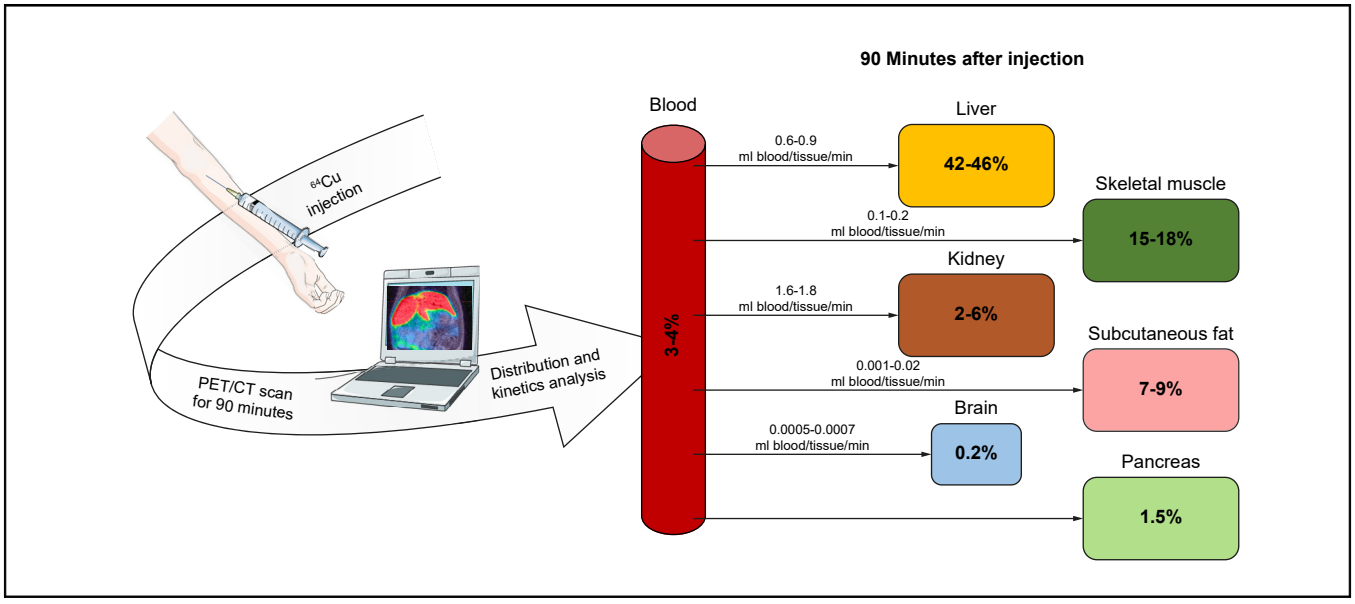

Highlights

- Following i.v. injection, ^{64}Cu quickly leaves the blood and is distributed to a number of tissues.
- Extrahepatic tissues account for 45-58% of ^{64}Cu 10 minutes after injection.
- Skeletal muscle may protect more sensitive organs from spikes in the non-ceruloplasmin-bound copper fraction.
- Kinetic analysis shows that exchange of ^{64}Cu from the blood to the brain is a very slow process.
- Better understanding of the exchange of copper between the blood and brain may reveal new targets for therapy.

Impact and implications

Maintaining non-ceruloplasmin-bound copper within the normal range is an important treatment goal in WD as this “free” copper is considered toxic to the liver and brain. We found that intravenously injected non-ceruloplasmin-bound copper quickly distributed to a number of tissues, especially skeletal muscle, subcutaneous fat, and the liver, while uptake into the brain was slow. This study offers new insights into the mechanisms of copper control, which may encourage further research into potential new treatment targets.

https://doi.org/10.1016/j.jhepr.2023.100916

Research article

JHEP|Reports

Distribution of non-ceruloplasmin-bound copper after i.v. ^{64}Cu injection studied with PET/CT in patients with Wilson disease

Ditte Emilie Munk,[1,*] Mikkel Holm Vendelbo,[2,3] Frederik Teicher Kirk,[1] Karina Stubkjær Rewitz,[1] Dirk Andreas Bender,[2] Karina Højrup Vase,[2] Ole Lajord Munk,[2] Hendrik Vilstrup,[1] Peter Ott,[1] Thomas Damgaard Sandahl[1]

[1]*Department of Hepatology and Gastroenterology, Aarhus University Hospital, Aarhus, Denmark;* [2]*Department of Nuclear Medicine and PET Centre, Aarhus University Hospital, Aarhus, Denmark;* [3]*Department of Biomedicine, Aarhus University, Aarhus, Denmark*

JHEP Reports **2023.** https://doi.org/10.1016/j.jhepr.2023.100916

Background & Aims: In Wilson disease (WD), copper accumulation and increased non-ceruloplasmin-bound copper in plasma lead to liver and brain pathology. To better understand the fate of non-ceruloplasmin-bound copper, we used PET/CT to examine the whole-body distribution of intravenously injected 64-copper (^{64}Cu).
Methods: Eight patients with WD, five heterozygotes, and nine healthy controls were examined by dynamic PET/CT for 90 min and static PET/CT up to 20 h after injection. We measured ^{64}Cu activity in blood and tissue and quantified the kinetics by compartmental analysis.
Results: Initially, a large fraction of injected ^{64}Cu was distributed to extrahepatic tissues, especially skeletal muscle. Thus, across groups, extrahepatic tissues accounted for 45-58% of the injected dose (%ID) after 10 min, and 45-55% after 1 h. Kinetic analysis showed rapid exchange of ^{64}Cu between blood and muscle as well as adipose tissue, with ^{64}Cu retention in a secondary compartment, possibly mitochondria. This way, muscle and adipose tissue may protect the brain from spikes in non-ceruloplasmin-bound copper. Tiny amounts of cerebral ^{64}Cu were detected (0.2%ID after 90 min and 0.3%ID after 6 h), suggesting tight control of cerebral copper in accordance with a cerebral clearance that is 2-3-fold lower than in muscle. Compared to controls, patients with WD accumulated more hepatic copper 6-20 h after injection, and also renal copper at 6 h.
Conclusion: Non-ceruloplasmin-bound copper is initially distributed into a number of tissues before being redistributed slowly to the eliminating organ, the liver. Cerebral uptake of copper is extremely slow and likely highly regulated. Our findings provide new insights into the mechanisms of copper control.
Impact and implications: Maintaining non-ceruloplasmin-bound copper within the normal range is an important treatment goal in WD as this "free" copper is considered toxic to the liver and brain. We found that intravenously injected non-ceruloplasmin-bound copper quickly distributed to a number of tissues, especially skeletal muscle, subcutaneous fat, and the liver, while uptake into the brain was slow. This study offers new insights into the mechanisms of copper control, which may encourage further research into potential new treatment targets.
Clinical trial number: 2016–001975-59.

Introduction

Wilson disease (WD) is a rare inherited disease in which mutations of the *ATP7B* gene cause dysfunction of the ATP7B protein.[1] The ATP7B protein is most abundantly expressed in the liver where it delivers copper to the trans-Golgi network and mediates either the irreversible incorporation of copper into ceruloplasmin or the export of excess copper into the bile which is the only way for the organism to remove excess copper.[2] ATP7B dysfunction leads to disease-causing accumulation of copper in the liver and elevated levels of non-ceruloplasmin-bound copper in the blood. This fraction of plasma copper (≈10% in healthy individuals) is loosely bound to albumin, other peptides, or amino acids[3] and is exchanged between blood and tissues. With time, elevated non-ceruloplasmin-bound copper in WD results in accumulation of copper in non-hepatic organs resulting in tissue injury, especially in the brain where the basal ganglia are most commonly affected. Clinically, patients with WD typically present with hepatic, neurologic and/or psychiatric symptoms.[4,5] Treatment of WD classically has two aims: removing excess copper from the body and maintaining non-ceruloplasmin-bound copper within the normal range.[6] Control of non-ceruloplasmin-bound copper is generally achieved in adherent patients,[7–9] and is used to monitor treatment efficacy in WD.[10,11]

While excess copper is toxic for cells,[12] the metal is also essential for numerous enzymatic processes in the human body, not least in the mitochondria.[13] The necessary tight control of plasma-organ exchange of copper is maintained by specific

Keywords: Tracer kinetics; NCC; free copper; whole-body distribution; bioavailable copper.
Received 30 June 2023; received in revised form 31 August 2023; accepted 31 August 2023; available online 25 September 2023
* Corresponding author. Address: Department of Hepatology and Gastroenterology, Aarhus University Hospital, Palle Juul-Jensens Boulevard 99, 8200 Aarhus N, Denmark.
E-mail address: dittmu@rm.dk (D.E. Munk).

copper-transporting proteins, such as copper transporter 1 (CTR1), ATP7A and ATP7B, with large variation between tissues.[14] The result is a carefully orchestrated distribution of non-ceruloplasmin-bound copper between blood and tissues. Even though the dynamics and kinetics of this distribution are important for our understanding of the pathophysiology of WD and the action of current and future treatments, a comprehensive description is not available.

Our aim was to study the distribution kinetics of non-ceruloplasmin-bound copper using the positron-emitting tracer $^{64}CuCl_2$ (^{64}Cu) and PET/CT scans.[15] The tracer has a half-life of 12.7 h allowing for both short and medium-term *in vivo* imaging of copper metabolism in cells, animals, and humans. The present study is a re-analysis of data from an earlier trial[15] that focused on the diagnostic aspects of ^{64}Cu PET/CT. Here, we specifically examined the distribution of non-ceruloplasmin-bound copper during the initial 90 min after intravenous injection of ^{64}Cu, *i.e.* before incorporation of the tracer into ceruloplasmin. We further examined the whole-body distribution 1.5, 6 and 20 h after injection. All analyses were performed in patients with WD, healthy controls and healthy persons who were heterozygous for a disease-causing *ATP7B* mutation. The study is the first of its kind in humans, including patients with WD.

Materials and methods

Ethics

All data was collected as part of the clinical trial "The pathophysiology of Wilson disease visualised: A human ^{64}Cu PET study" (EudraCT 2016–001975-59).[15] The study was approved by the Regional Ethics Committee in Central Denmark Region and the Danish Medicines Agency, conducted in accordance with the Helsinki II Declaration, and monitored by the Unit for Good Clinical Practice at Aarhus and Aalborg University Hospitals.

Study design

The trial involved three groups: patients with Wilson disease (WDP), healthy persons who were heterozygotes for a disease-causing *ATP7B* mutation (parents, children, or heterozygote siblings to WDP [HZ]) and healthy controls who were assumed not to be carriers of a disease-causing *ATP7B* mutation (CON). The study design has been described in detail elsewhere.[15] Briefly, participants fasted for a minimum of 8 h before the first scan (water allowed). WDP abstained from WD treatment for 3 days prior to the first scan. After intravenous (i.v.) administration of 55-75 megabecquerel (MBq) of ^{64}Cu, its distribution was followed in one dynamic (continuous) PET scan of 90 min, then three static scans each lasting 10 min after 1.5, 6 and 20 h.

Participants

Nine WDP diagnosed according to the Leipzig criteria[5] were recruited at the Department of Hepatology, Aarhus University Hospital at outpatient visits. Five HZ were recruited among WDP relatives, and eight CON through a local newspaper advertisement.

Inclusion criteria were age ≥18 and safe contraception for females. Exclusion criteria for WDP were decompensated cirrhosis, model for end-stage liver disease score >11 or modified Nazer score >6.[16,17] Exclusion criteria for all participants were known hypersensitivity to ^{64}Cu or other ingredients in the tracer formula, pregnancy, breastfeeding, or a desire to become pregnant before the end of the trial. All participants signed informed consent before enrolling in the study.

Radiochemistry

The ^{64}Cu radioisotope was obtained from a commercial source (Hevesy Laboratory, DTU Nutech, Risø, Roskilde, Denmark). The ^{64}Cu tracer solution (a sterile acetate-buffered solution of $^{64}CuCl_2$) was subsequently prepared and quality controlled at our centre, as previously described.[15]

PET/CT scans

The scanning methods have been described elsewhere.[15] Briefly, participants were placed supinely in a Siemens Biograph™ 64 TruePoint™ PET/CT camera with the liver within the 21.6 cm axial field-of-view. A low dose CT scan was performed before each PET scan for definition of anatomical structures and attenuation correction of the PET recordings. The ^{64}Cu solution was administered as an intravenous bolus injection over the course of 10 s (median dose 72.9 MBq, range 53-77 MBq) followed by a 90-minute dynamic PET scan of the liver. Then, three consecutive whole-body PET/CT scans of 10-minute duration were performed at 1.5, 6, and 20 h after tracer administration. The PET images were reconstructed using 3D ordered-subset expectation maximization with four iterations and 21 subsets, 4-mm Gauss filter, and 168 × 168 matrix with voxel size 4 × 4 × 5 mm^3.

Image analysis

PET data was assessed using PMOD (version 4.0, PMOD Technologies LLC). The amount of ^{64}Cu in an organ was measured by the mean radioactivity (kBq/ml) in a volume of interest (VOI) with a size appropriate for the organ, *i.e.* VOIs of 30-40 cm^3 in muscle, 15 cm^3 in the brain, and 0.5 cm^3 in pancreas. In organs with large heterogeneity of tracer distribution (*e.g.*, the colon lumen), the mean of 3-4 VOIs was used, because large VOIs were difficult to define. Within the field-of-view for the dynamic scans, it was possible to assess activity in blood (aorta), liver, gallbladder, kidneys, pancreas, colon, skeletal muscle, subcutaneous fat, bone marrow, heart, and lung. The brain and bladder were only available on the static scans, at 1.5, 6 and 20 h after injection, as the dynamic scan was restricted by a 21.6 cm field-of-view over the liver.

Data analysis

To describe the distribution of ^{64}Cu in organs, the percentage of injected dose (%ID) in each organ was calculated after correction for decay and by multiplying the radioactivity per ml of organ tissue by the estimated tissue size under the assumption that the radioactivity was homogenously distributed in the organ. The size of the organ was either determined as a standard size[18] or calculated by formulas for liver,[19,20] skeletal muscle[21,22] and body fat[23] (Tables S1 and S2).

Kinetic analysis

The kinetic parameters were obtained using PMOD (version 4.0, PMOD Technologies LLC). The analyses were performed in each individual and mean ± standard deviation of each group is presented. Kinetic parameters were obtained by fitting one-, two- and three-tissue compartment kinetic models to the dynamic PET data with aorta activity as the input function (reference tissue) for the whole blood pool. In separate analyses, liver, skeletal muscle, kidney, and subcutaneous fat time activity curves were used to examine the kinetics of blood-tissue

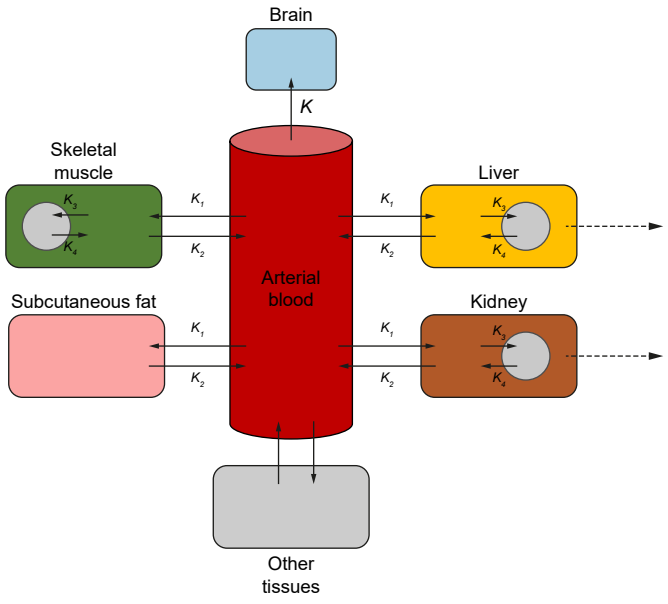

Fig. 1. Principles of the kinetic analysis.

exchange of ^{64}Cu. The goodness of fit was evaluated by the Akaike information criterion, which takes into account that inclusion of more variables will reduce the degrees of freedom. The physiologically plausible compartment model with the lowest Akaike information criterion value was chosen as the best fit. For liver, kidney and skeletal muscle, two-tissue compartment models with reversible exchange between blood and tissue and reversible exchange between a second compartment within the tissue provided the best fit (Fig. S1). With such a model, the exchange of ^{64}Cu between blood and tissue is determined by the clearance per ml tissue, K_1 (ml blood · ml tissue · min^{-1}) and the rate constant for back flux from tissue to blood, k_2 (min^{-1}) describing the fraction of exchangeable ^{64}Cu in the tissue that is returned to the blood per minute (see Fig. 1). The trapping and release of ^{64}Cu in a second ("deep") compartment within the tissue is determined by k_3 (min^{-1}) and k_4 (min^{-1}), respectively (see Fig. 1). For subcutaneous fat, a one-tissue compartment model with reversible exchange between blood and tissue provided the best fit (see Fig. 1).

Uptake of ^{64}Cu from the blood to the brain is of particular clinical interest in WD. Because data were only available from the static scans, we estimated the clearance per ml of tissue or the net influx rate, K, with calculation of the fractional uptake rate[24] at 90 min after injection assuming only influx of ^{64}Cu from the blood to the brain.

$$K(t = 90\ min) = \frac{Activity\ in\ brain\ (t = 90\ min)}{AUC\ in\ blood\ (0\text{–}90\ min)}$$

where activity in the brain at 90 min after injection is per ml of brain tissue and the area under the curve is the area under the blood time activity curve from time 0 to 90 min.

Results

The study included nine WDP, five HZ, and eight CON. Demographics are shown in Table 1. There were no statistically significant differences regarding gender, age, or body mass index.

The blood time activity curves are displayed in Fig. 2A (activity displayed as %ID in blood), and the distribution over time of %ID in the various organs in Fig. 3 and Table 2.

Blood

The blood time activity curves were similar in the three groups (Fig. 2A). After 2 min, the injected dose was well mixed in the blood volume and significant distribution to different organs was already detectable, since the blood activity was reduced to 30-40%ID after 2 min (Fig. 2A and Table 2). After the fast initial distribution phase, the blood activity declined more slowly to reach around 20%ID at 10 min, indicating that ≈80% of the dose had been distributed to various organs (Fig. 2A and Fig. 3). At the early time points, the total %ID sums up to slightly more than 100% (Fig. 3), likely because calculations do not account for blood content in the individual organs, not to mention uncertainties caused by the short initial time frames and calculated organ sizes that may not be entirely correct.

Twenty hours after injection, ^{64}Cu blood activity was significantly higher in CON (4.04 ± 1.15%ID) than in WDP (1.42 ± 1.49%ID) with intermediate values in HZ (2.70 ± 1.62%ID) (Table 2, Fig. 2B). This likely reflects the hepatic secretion of ceruloplasmin-bound ^{64}Cu in CON and HZ which is absent in WD. This was further underlined by a correlation analysis of ceruloplasmin concentrations in plasma and %ID in blood at 20 h, which correlated strongly (Pearson's rho = 0.6, p = 0.009) across groups but not within groups (Fig. S3).

Table 1. Demographics.

	Patients with WD	Heterozygotes	Healthy controls
Gender (male/female)	7/2	3/2	3/5
WD treatment			
Penicillamine	6		
Trientine	1		
Zinc	2		
WD presentation			
Hepatic	6		
Neurologic	1		
Asymptomatic sibling	1		
Age, years, mean ± SD	44.4 ± 8.5	35.2 ± 18.5	35.9 ± 17.6 (n.s.)
BMI, mean ± SD	23.7 ± 3.1	22.6 ± 1.1	27.0 ± 4.5 (n.s.)
Tracer dose, MBq, mean ± SD	70.8 ± 7.4	70.7 ± 4.2	72.4 ± 3.6 (n.s.)

Values are n or mean ± standard deviation.
n.s. = p >0.05 (one-way ANOVA).
WD, Wilson disease.

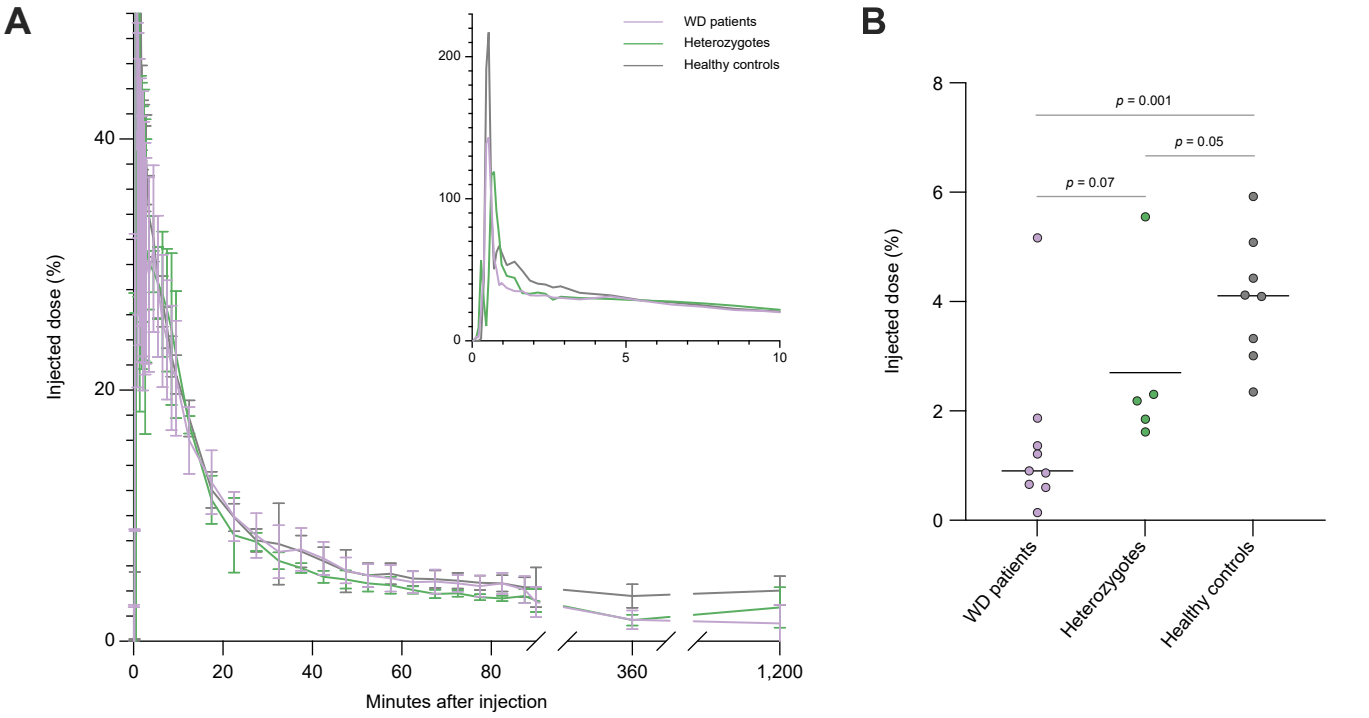

Fig. 2. Blood %ID. (A) 0-90 min after injection, inserted graph: 0-10 min after injection (mean values) (B) Dot plot of blood %ID at 20 h after injection (lines indicate mean values, Student's t-test). %ID, percentage of injected dose; WD, Wilson disease.

To further explore the extensive extravascular distribution of ^{64}Cu, we followed the activity over time in several organs (Fig. 3, Table 2, Fig. S2A-I). There was some distribution of ^{64}Cu to most organs, but predominantly to the liver, skeletal muscles, subcutaneous fat, kidneys, and pancreas.

Liver

The ^{64}Cu content in the liver was ≈10%ID at 2 min, ≈25 %ID at 10 min and then steadily increased to ≈ 45%ID at 90 min (Fig. 3A,C,E, Table 2, Fig. S2A) with no difference between the groups. After 6 h, the hepatic %ID was slightly higher in WDP (52.1 ± 4.6%) and HZ (55.1 ± 6.2%) compared to CON (44.6 ± 7.6%) (Table 2). After 20 h, the liver content continued to increase in WDP (65.0 ± 7.7%), was stable in HZ (52.5 ± 6.7%), and decreased in CON to 39.2 ± 12.1%. These late differences have been described by Sandahl *et al.*[15] and reflect that ^{64}Cu is trapped in the liver in WDP, since it cannot be excreted to bile or incorporated into ceruloplasmin. It further demonstrates that the biliary excretion of ^{64}Cu is slower in HZ than in CON.

Skeletal muscle

There was a very fast distribution of ^{64}Cu from the blood to the skeletal muscle tissue. Already 2 min after injection, 40-45% of the injected dose was in skeletal muscle tissue in all groups (Table 2, Fig. 3, Fig. S2H). That increased to a maximum after 10 min, where muscle %ID was higher in WDP (57.8 ± 17.5%) and HZ (59.8 ± 15.0%) than in CON (47.7 ± 17.5%), though the difference was not statistically significant. From that time point, muscle %ID slowly decreased to 16-23% at 20 h. Thus, skeletal muscle acted as a temporary store for ^{64}Cu.

Subcutaneous fat

Subcutaneous fat contained measurable amounts of ^{64}Cu after 20-30 s, increasing to a maximum of 10-15%ID after 10 min (Fig. 3, Table 2, Fig. S2G). After 20 h, 3-6% of the injected dose was still in subcutaneous fat. Thus, subcutaneous fat, like skeletal muscle, acted as a quantitatively important temporary store for ^{64}Cu. At 20 h after injection, the %ID was significantly higher in CON compared to WDP and HZ (one-way ANOVA, p = 0.02, Table 2).

Kidneys

During the initial 2-minute period, the kidneys absorbed approximately 4-5% of the administered dose. In the WDP group, this proportion remained relatively constant for the first 90 min, whereas it gradually declined in the HZ and CON groups (Fig. 4). At 6 h after injection, the %ID in the kidneys was higher in WDP (6.3 ± 6.0%) than in HZ (1.6 ± 0.4%) and CON (1.6 ± 0.2%) (one-way ANOVA, p <0.001).

Bladder ^{64}Cu activity was only measurable on the static scans (1.5, 6 and 20 h after injection), and was low but significantly higher after 6 h in WDP compared to HZ and CON (one-way ANOVA, p <0.001) (Table 2).

Pancreas

Copper activity reached a maximum of 1.2-1.4%ID shortly after injection (around 3 min) and slowly declined to ≈1%ID after 6 h,

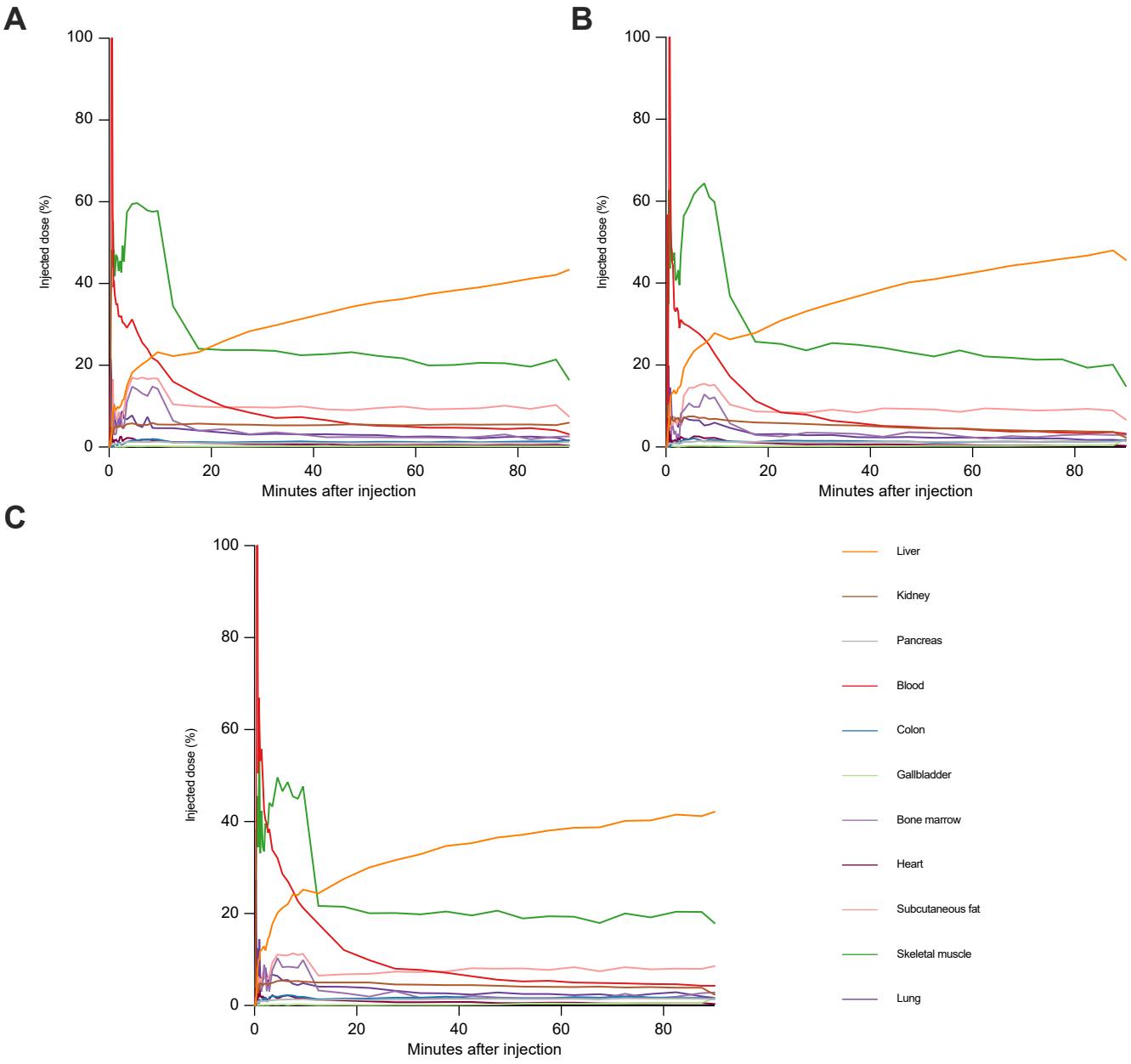

Fig. 3. All organs %ID (mean values). (A) WDP, 0-90 min after injection. (B) HZ, 0-90 min after injection. (C) CON, 0-90 min after injection. %ID, percentage of injected dose; CON, healthy controls; HZ, heterozygous relatives of WDP; WDP, patients with Wilson disease.

and ≈0.5%ID after 20 h (Fig. 3, Table 2, Fig. S2B). There were no group differences.

Brain

The brain was only accessible on the static scans (1.5, 6 and 20 h after injection). The brain parenchymal activity was low but detectable after correction for activity in blood that was assumed to take up 4% of the cerebral VOIs.[25]

After this correction, the cerebral %ID was 0.15%-0.22% at 1.5 h after injection, increasing to 0.28%-0.33% after 6 h, and 0.29%-0.36% after 20 h (Table 2, Fig. 5).

At the 1.5-hour time point, cerebral ^{64}Cu levels tended to be higher in WDP and HZ than in CON (Fig. 5A), but no significant differences were detected.

Kinetic analyses

To explore the kinetics behind these observations, we performed kinetic analyses of the ^{64}Cu exchange between organ and blood in the most relevant tissues: skeletal muscle, kidney, subcutaneous fat, and brain (Table 3).

Liver

We used a two-tissue compartment model as it provided the best fit for 19/22 participants.

K_1, k_2 and k_3 did not differ significantly between the groups but k_4 was significantly lower in WDP and HZ compared to CON (one-way ANOVA, p <0.001, Table 3). A low k_4 indicates trapping in a second compartment, *i.e.*, a deep intracellular compartment (Fig. 1). K_1 in WDP was 0.58 ± 0.30 ml/cm^3/min, in HZ 0.89 ±

Table 2. %ID in patients with WD, heterozygotes and healthy controls at different time points over 20 h.

	Patients with WD	Heterozygotes	Healthy controls	Patients with WD	Heterozygotes	Healthy controls
	Blood			**Liver**		
10 s	2.28 ± 6.64	9.26 ± 18.49	0.07 ± 0.10	1.60 ± 1.39	0.38 ± 0.81	0.42 ± 0.45
20 s	51.65 ± 6.64	27.49 ± 54.89	44.12 ± 49.82	1.74 ± 1.15	2.49 ± 2.15	2.13 ± 2.35
2 min	32.04 ± 14.08	33.10 ± 11.43	42.49 ± 3.39	9.55 ± 1.51	13.04 ± 2.14	12.86 ± 3.26*
10 min	20.97 ± 4.59	22.82 ± 5.08	21.24 ± 1.54	23.20 ± 3.88	27.83 ± 3.54	25.22 ± 9.85
90 min	3.13 ± 1.20	3.24 ± 0.93	4.31 ± 1.58	43.37 ± 3.80	45.67 ± 6.76	42.15 ± 6.40
6 h	1.72 ± 0.75	1.70 ± 0.44	3.60 ± 0.95***	52.10 ± 4.57	55.12 ± 6.24	44.58 ± 7.61*
20 h	1.42 ± 1.49	2.70 ± 1.62	4.04 ± 1.15**	64.93 ± 7.66	52.52 ± 6.68	39.24 ± 12.09***
	Kidneys (pair)			**Pancreas**		
10 s	0.01 ± 0.03	0.12 ± 0.26	0.03 ± 0.09	0.02 ± 0.05	0.00 ± 0.00	0.01 ± 0.02
20 s	2.53 ± 2.44	4.01 ± 4.67	1.53 ± 1.82	0.66 ± 0.48	0.64 ± 0.64	0.46 ± 0.46
2 min	2.87 ± 1.25	7.11 ± 3.16	4.73 ± 1.28	0.80 ± 0.28	0.98 ± 0.47	0.96 ± 0.29
10 min	5.53 ± 1.19	6.92 ± 2.61	5.21 ± 1.38	1.33 ± 0.27	1.34 ± 0.37	1.40 ± 0.56
90 min	5.98 ± 3.69	2.32 ± 0.55	2.38 ± 0.53***	1.30 ± 0.58	1.50 ± 0.53	1.44 ± 0.67
6 h	6.30 ± 6.00	1.56 ± 0.41	1.60 ± 0.22***	0.93 ± 0.44	0.99 ± 0.19	1.08 ± 0.59
20 h	1.76 ± 0.51	1.29 ± 0.23	1.45 ± 0.25	0.47 ± 0.22	0.46 ± 0.33	0.60 ± 0.34
	Colon (lumen and intestinal wall)			**Heart muscle**		
10 s	0.00 ± 0.00	0.00 ± 0.00	0.00 ± 0.00	3.14 ± 3.71	2.10 ± 3.57	1.84 ± 2.62
20 s	0.24 ± 0.03	0.14 ± 0.31	0.08 ± 0.21	4.78 ± 3.69	3.47 ± 3.74	3.77 ± 3.95
2 min	1.29 ± 1.06	0.95 ± 0.58	1.04 ± 1.52	1.25 ± 1.04	1.65 ± 1.18	1.52 ± 0.51
10 min	1.89 ± 0.82	1.64 ± 0.51	1.92 ± 1.94	1.58 ± 0.86	2.24 ± 1.06	1.65 ± 0.81
90 min	1.66 ± 0.32	1.65 ± 0.41	1.42 ± 0.56	0.32 ± 0.09	0.27 ± 0.06	0.38 ± 0.11
6 h	2.12 ± 0.75	2.19 ± 0.99	3.78 ± 1.72*	0.22 ± 0.07	0.20 ± 0.06	0.25 ± 0.08
20 h	2.12 ± 0.73	3.26 ± 1.42	5.84 ± 2.53**	0.19 ± 0.06	0.26 ± 0.12	0.29 ± 0.15
	Gallbladder			**Bone marrow**		
10 s	0.00 ± 0.00	0.00 ± 0.00	0.00 ± 0.00	0.01 ± 0.02	0.00 ± 0.00	1.77 ± 5.02
20 s	0.06 ± 0.07	0.02 ± 0.03	0.05 ± 0.09	1.28 ± 3.10	0.03 ± 0.07	4.41 ± 10.06
2 min	0.13 ± 0.12	0.11 ± 0.07	0.10 ± 0.10	5.40 ± 5.97	3.95 ± 4.34	8.89 ± 9.61
10 min	0.22 ± 0.11	0.31 ± 0.17	0.21 ± 0.17	14.26 ± 9.05	12.12 ± 6.40	9.91 ± 9.58
90 min	0.20 ± 0.14	1.94 ± 3.46	1.64 ± 1.50**	2.61 ± 0.60	3.00 ± 0.89	2.83 ± 1.24
6 h	0.26 ± 0.18	0.73 ± 0.53	1.43 ± 0.96*	2.06 ± 1.06	2.44 ± 0.59	4.21 ± 1.33**
20 h	0.22 ± 0.16	2.34 ± 2.59	1.18 ± 0.66	1.72 ± 0.86	1.88 ± 0.45	4.26 ± 1.47***
	Bladder (content)			**Brain**		
90 min	0.53 ± 0.23	0.18 ± 0.13	0.14 ± 0.06***	0.21 ± 0.08	0.22 ± 0.10	0.15 ± 0.08
6 h	0.27 ± 0.19	0.11 ± 0.06	0.17 ± 0.08	0.33 ± 0.06	0.30 ± 0.03	0.28 ± 0.12
20 h	0.11 ± 0.06	0.06 ± 0.06	0.13 ± 0.03	0.29 ± 0.09	0.36 ± 0.08	0.36 ± 0.16
	Subcutaneous fat			**Skeletal muscle**		
10 s	0.00 ± 0.00	0.04 ± 0.08	0.54 ± 1.53	3.11 ± 4.32	2.99 ± 6.65	1.33 ± 1.58
20 s	1.32 ± 2.08	0.19 ± 0.41	0.43 ± 0.63	33.93 ± 30.29	17.61 ± 14.06	38.37 ± 30.32
2 min	8.59 ± 6.12	6.81 ± 4.35	7.36 ± 5.95	43.09 ± 15.65	40.66 ± 10.10	33.53 ± 11.98
10 min	16.74 ± 9.20	15.17 ± 7.39	11.21 ± 5.01	57.79 ± 17.47	59.81 ± 14.99	47.65 ± 17.51
90 min	7.48 ± 3.55	6.68 ± 1.60	8.60 ± 4.28	16.49 ± 3.53	14.86 ± 1.61	17.89 ± 5.16
6 h	5.01 ± 2.31	4.33 ± 1.49	7.97 ± 5.62	14.50 ± 1.79	13.92 ± 2.37	17.58 ± 4.75
20 h	2.78 ± 1.27	2.68 ± 0.69	5.90 ± 3.67*	13.83 ± 4.77	14.79 ± 2.65	16.75 ± 5.29
	Lungs					
10 s	16.23 ± 25.01	9.43 ± 12.01	12.28 ± 12.61			
20 s	21.02 ± 13.53	21.30 ± 20.46	16.23 ± 13.63			
2 min	7.04 ± 4.20	5.97 ± 3.25	6.47 ± 4.20			
10 min	4.62 ± 3.19	5.94 ± 1.60	4.89 ± 2.46			
90 min	1.55 ± 0.66	1.57 ± 0.43	1.67 ± 0.77			
6 h	0.96 ± 0.40	1.09 ± 0.58	1.56 ± 0.67			
20 h	0.66 ± 0.30	1.25 ± 0.33	1.53 ± 0.81*			

Values presented are mean ± standard deviation.
*p <0.05 (one-way ANOVA), **p <0.01 (one-way ANOVA), ***p <0.001 (one-way ANOVA).

0.66 ml/cm^3/min and in CON 0.77 ± 0.51 ml/cm^3/min, which was not significantly different.

Skeletal muscle kinetics

A two-tissue compartment model was the best fit for all participants (Fig. S1). K_1, k_2, k_3 and k_4 did not differ significantly between the groups (Table 3). For all participants combined, K_1 was 0.19 ± 0.15 ml/cm^3/min, k_2 0.76 ± 0.39 min^{-1}, k_3 0.015 ± 0.011 min^{-1} and k_4 0.0045 ± 0.0079 min^{-1}.

Kidney kinetics

A two-tissue compartment model was the best fit for all participants except one with clearly deviating values (one HZ) who was excluded from the analysis. K_1, k_2 and k_3 did not differ

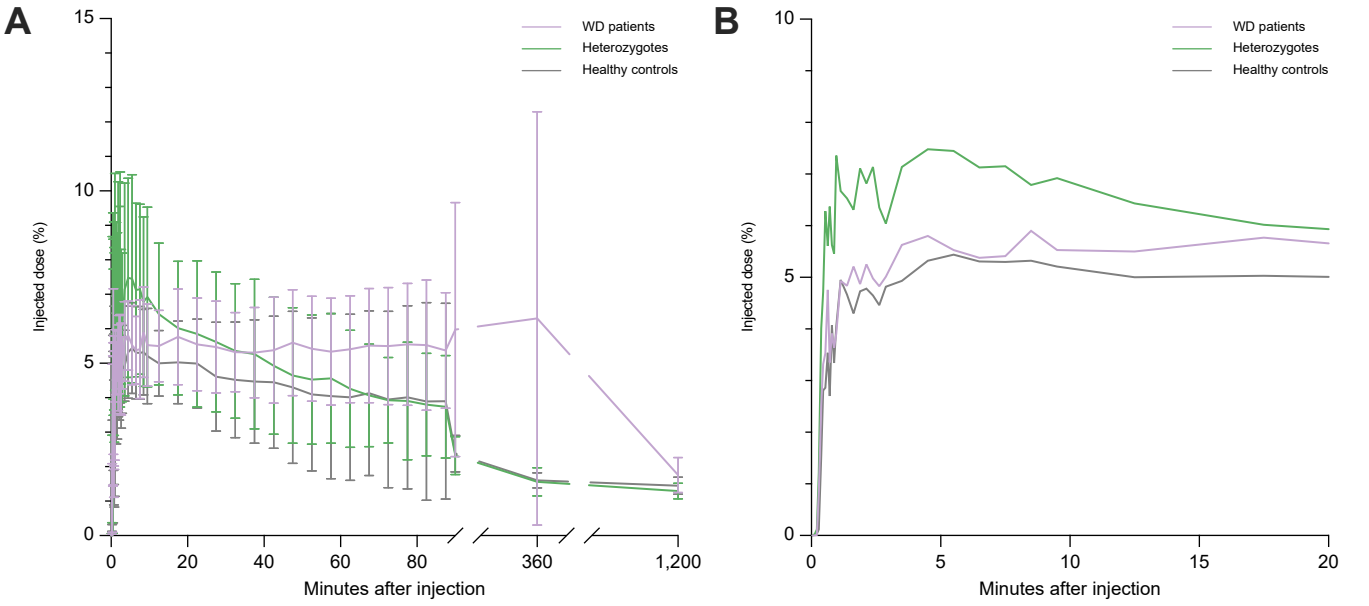

Fig. 4. Kidney %ID. %ID, percentage of injected dose; WD, Wilson disease.

significantly between the groups (Table 3). WDP and HZ had significantly lower k_4 than CON (Kruskal-Wallis test, p <0.0001, Table 3), suggesting a higher degree of trapping in a second renal compartment in WDP and HZ.

Subcutaneous fat

A one-tissue compartment model provided the best fit for all participants except one WDP for whom a two-tissue compartment model was more accurate. K_1 and k_2 were an order of magnitude lower than with skeletal muscle and did not differ between the groups (Table 3).

Brain kinetics

Brain activity could not be followed dynamically for the first 90 min, so we only report activities measured at the static scans at 90 min after injection. At the 90-minute time point, before ceruloplasmin-bound ^{64}Cu arrived in the blood stream, we calculated the net influx rate K based on the net uptake of ^{64}Cu into the brain during the first 90 min. As seen in Table 3, there was a trend that K was higher in WDP than in CON with intermediate values in HZ. These data demonstrate that non-ceruloplasmin-bound copper can enter the brain, although at a very low rate compared to other organs.

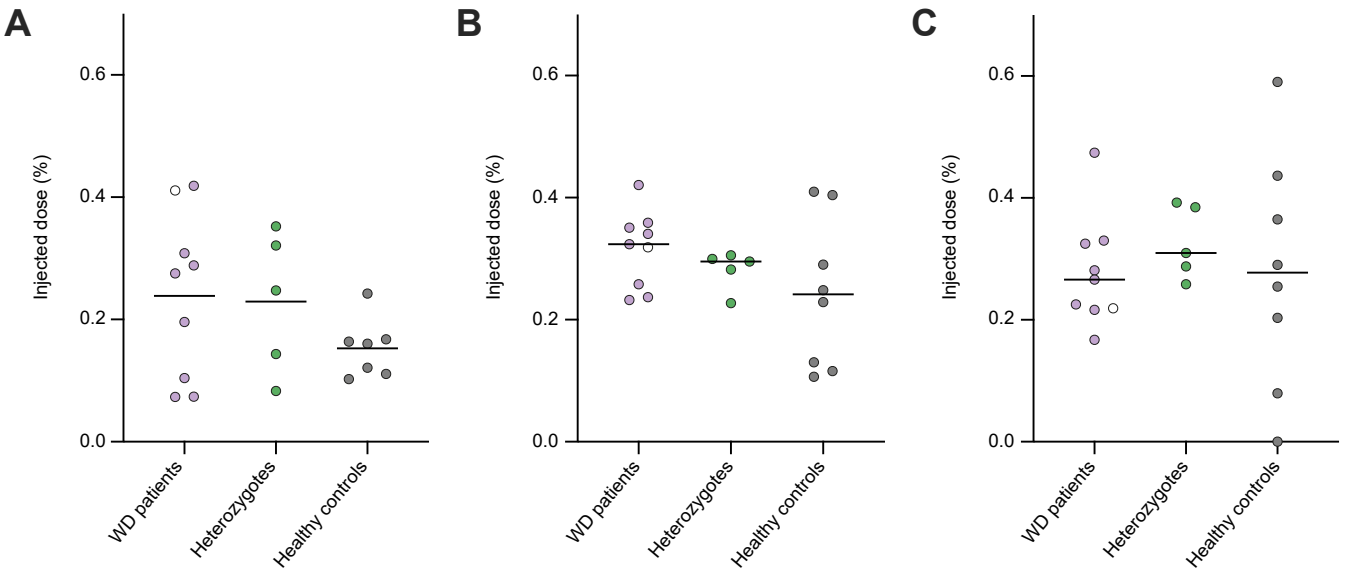

Fig. 5. Brain %ID attributable to brain parenchyma copper levels. (A) 1.5 h after injection (B) 6 h after injection (C) 20 h after injection (lines indicate mean values, no significant differences (One-way ANOVA), white dot indicates patient with neurological phenotype). %ID, percentage of injected dose; WD, Wilson disease.

Table 3. Kinetic parameters K_1, k_2, k_3 and k_4.

	K_1ˆ	$k_2^{\otimes}$	$k_3^{\otimes}$	$k_4^{\otimes}$
Liver				
Patients with WD	0.58 ± 0.30	0.42 ± 0.25	0.108 ± 0.039	0.0017 ± 0.0018*
Heterozygotes	0.89 ± 0.66	0.69 ± 0.54	0.132 ± 0.056	0.0011 ± 0.0018*
Healthy controls	0.77 ± 0.51	0.54 ± 0.37	0.128 ± 0.038	0.010 ± 0.0062*
Skeletal muscle				
Patients with WD	0.21 ± 0.18	0.77 ± 0.47	0.013 ± 0.006	0.0034 ± 0.0086
Heterozygotes	0.18 ± 0.14	0.71 ± 0.37	0.017 ± 0.012	0.0057 ± 0.009
Healthy controls	0.14 ± 0.07	0.72 ± 0.29	0.016 ± 0.014	0.0054 ± 0.0077
Kidneys				
Patients with WD	1.82 ± 0.83	1.09 ± 0.44	0.058 ± 0.019	0.0087 ± 0.0057*
Heterozygotes	1.82 ± 0.77	1.10 ± 0.50	0.050 ± 0.015	0.015 ± 0.0039*
Healthy controls	1.57 ± 0.62	0.89 ± 0.39	0.056 ± 0.019	0.028 ± 0.0095*
Subcutaneous fat				
Patients with WD	0.022 ± 0.041	0.16 ± 0.41		
Heterozygotes	0.0046 ± 0.0032	0.013 ± 0.010		
Healthy controls	0.0015 ± 0.00186	0.0043 ± 0.0073		
	Brain (1.5 h after injection)			
	Kˆ			
Patients with WD	0.00090 ± 0.00053			
Heterozygotes	0.00085 ± 0.00029			
Healthy controls	0.00067 ± 0.00018			

Values presented are mean ± standard deviation.
ˆ = ml blood · ml tissue · min−1, ⊗ = min^{-1}, *p <0.05 (one-way ANOVA).

Discussion

In this ^{64}Cu PET/CT study, which is the first of its kind in humans including WDP, HZ and CON, we investigated the distribution of non-ceruloplasmin-bound copper during the 90 min after an i.v. injection. The initial clearance of ^{64}Cu from the blood to tissues was similar between WDP, HZ and CON. Injected ^{64}Cu distributed to a number of tissues, especially the liver (23-28% after 10 min), skeletal muscle (50-60% after 10 min), and subcutaneous fat (11-17% after 10 min). After 90 min, a large part was redistributed to the eliminating organ, the liver (42-46% after 90 min), but more than 50% of injected ^{64}Cu remained in extrahepatic tissues. At later time points, ^{64}Cu was more slowly released from extrahepatic tissues to the blood for further hepatic elimination in CON and HZ or accumulation in WDP. Thus, extrahepatic tissue and especially the muscles, acted as a temporary storage for non-ceruloplasmin-bound copper.

Cerebral uptake of small amounts of ^{64}Cu was detectable at 1.5, 6 and 20 h after injection, with a tendency to higher levels in WDP and HZ compared to CON 1.5 h after injection. Kinetic analysis illustrated that cerebral uptake of ^{64}Cu from the blood was a much slower process than with other organs, indicating very tight regulation of cerebral copper content.

Intravenous ^{64}Cu may be used for the diagnosis of WD[26,27] because it leaves the blood stream, with a minimum at around 2 h after injection, and then slowly returns in healthy individuals because of ceruloplasmin formation, peaking at 48 h after injection.[28] This “second peak” of ceruloplasmin is absent or much smaller in WDP, while HZ produce intermediate results.[27,28] In accordance, we observed initial removal of ^{64}Cu from the blood stream in all groups, while activity in blood and blood-rich tissues was higher in CON than in WDP, with intermediate values in HZ, 20 h after injection (Table 2).

An important finding in the present study was the temporary distribution of copper in extrahepatic tissues, where muscle and subcutaneous fat were quantitatively the most important. There are only a few studies for comparison, all in rodents. Owen used i.v. or per oral administration of ^{64}Cu in rats[29,30] and reported ≈45% of the dose in extrahepatic tissues after 20 min, mostly muscles and skin; subcutaneous fat was not assessed. Another study in wild-type rats reported ≈20% of injected ^{64}Cu in the liver, and ≈20% in muscles and skin after 5 min.[31] Peng *et al.* used i.v. injected ^{64}Cu and micro PET/CT in wild-type and *Atp7b* knockout mice and observed distribution into skeletal muscle, but only reported ^{64}Cu content in the liver, kidneys, lungs, heart and brain.[32] Weiss used intraperitoneal ^{67}Cu in rats, and observed redistribution to muscle, although somewhat delayed, possibly because of the route of administration and the use of a high dose of copper (0.33 μg/rat compared to 0.005 μg/person in the present study).[33] Thus, these reports from animal studies support our data.

The kinetic analysis of the exchange between blood and muscle supported this view. With K_1 of 0.19 ± 0.15 ml blood per cm^3 of muscle tissue per minute and a skeletal muscle volume of 30 L, the muscular clearance of non-ceruloplasmin-bound copper would equal 5.7 L of blood per minute to the fast-exchanging muscular copper pool, which is likely the myocyte cytosol. Since k_2 was 0.76 ± 0.39 min^{-1}, 76% of cytosolic copper was delivered back to the blood every minute. The much smaller rate constants k_3 and k_4 describe slower exchange between the cytosol and a second cellular compartment. We speculate that this second compartment may represent copper in mitochondria, which are abundant in muscle tissue. Kinetically speaking, trapping of ^{64}Cu in the second compartment slowed down exchange between muscles and blood, and prolonged the period in which muscles could buffer non-ceruloplasmin-bound copper.

The muscles are equipped with mechanisms for fast copper exchange, since copper is removed from the blood during exercise and released back again during rest,[34] presumably reflecting the varying mitochondrial needs. The net effect of this temporary distribution is a kind of buffer that reduces the exposure of other organs, including the brain, to copper. Unlike in muscle, it was not possible to identify a second compartment in subcutaneous fat, maybe owing to the presence of fewer mitochondria.

In normal physiology, the liver is the only organ that eliminates excess copper sufficiently to maintain copper balance. The

kinetic analysis of the exchange of ^{64}Cu between the blood and the liver was best fitted by a two-tissue compartment model as illustrated. In our previous publication,[15] liver kinetics modelling was applied to this data using the Gjedde-Patlak plot[15] which computes a constant *K* that describes the overall removal of ^{64}Cu from the blood by the liver. *K* was significantly lower in WDP compared to HZ and CON. In the present study, we were specifically interested in the initial clearance, K_1, and wanted to compare the kinetic parameters across organs, which dictated the slightly different approach with reporting of parameters from the two-tissue compartment analysis. K_1 tended to be lower in WDP compared to HZ and CON but the difference did not reach statistical significance. A lower K_1 could be related to CTR1 downregulation. CTR1 is the major transporter of copper into hepatocytes[35] and its activity is downregulated by internalization when copper levels are high as expected in WDP.[14,36–38]

The mean K_1 for all participants was 0.74 ± 0.63 ml blood per cm^3 of liver tissue per minute. With a liver of 1,500 ml, a K_1 around 0.75 ml blood per cm^3 of liver tissue per minute equals a hepatic ^{64}Cu clearance of 1.1 L/min, close to the hepatic blood flow. In our study, k_2 was around 0.5 min^{-1} suggesting significant back flux from the liver to the plasma, and measurable k_3 and k_4 demonstrates that a fraction of cytosolic ^{64}Cu was trapped in a second compartment with much slower exchange of ^{64}Cu. This second compartment could represent binding to metallothionines, since induction of metallothionein may be an important defense mechanism in WD.[3,31,39] Lower k_4 in WD could also represent trans-Golgi network trapping, since ATP7B is involved in incorporation of copper into ceruloplasmin or biliary excretion. Within the time frame of 90 min, k_3 and k_4 are most likely not affected by biliary excretion (only tiny amounts of ^{64}Cu could be measured in the gallbladder of CON at this time, Table 2).

The brain is susceptible to excess copper in WD, and at the same time, copper is essential for several brain functions.[40] After correction for activity in cerebral blood vessels, a small fraction of the injected dose ≈0.3% was recovered in the brain parenchyma at later time points. The estimated *K* was two orders of magnitude lower than for other organs, confirming tight regulation of cerebral copper with slow exchange between the blood and tissue. In accordance with earlier reports of elevated cerebrospinal copper in WDP,[41] there was an interesting trend that cerebral copper influx was higher in WDP than in healthy participants. A similar finding was suggested in a study from 1965 including two WDP and six controls and external gamma-detection.[42] The choroid plexus (with expression of CTR1 and ATP7A) plays a protective/homeostatic role in regulating brain copper levels, while the influx from the blood to the parenchyma is mainly through the capillary bed (with expression of CTR1 and ATP7B).[43] ATP7B may be involved in re-exporting endothelial copper to plasma.[44] Thus, the net influx of copper into the brain could theoretically be affected by ATP7B dysfunction in WD. Our results should stimulate further explorations of the blood-brain exchange of copper and the role of ATP7B. In general, little is known about copper's toxic effects on the brain, including the cause of neurological worsening following treatment initiation. Brain MRI pathology is well-established and widely used[45] and PET/MRI with flour-deoxyglucose shows that WDP with neurologic symptoms have reduced cerebral and striatal glucose metabolism,[46–48] and SPECT (single-photon emission computerized tomography) scans show reduced dopamine D2 receptor binding in the striatum.[49–51] Both abnormalities improve with de-coppering therapy. Indeed, more studies on copper fluxes and copper deposition in the human brain are warranted to explain why not all WDP develop neurologic symptoms and why current treatments do not always prevent brain disease progression in WD.

We speculate that future therapeutic targets could be the inhibition of cerebral influx or stimulation of efflux of cerebral copper.

The renal uptake of ^{64}Cu was similar initially but the %ID was higher in WD (6.3 ± 6.0%) than in HZ and CON (both below 2%) at 90 min. These differences were eliminated after 20 h (Table 2). Rodent studies reported similar findings.[32,52,53] ATP7B is expressed in the kidneys and involved in vesicular export of copper to urine.[54] Renal CTR1 is not downregulated in *Atp7b* knockout mice,[52] and lack of ATP7B function is a possible cause of temporary copper accumulation even though trafficking of ATP7A may partly compensate for this.[54] The temporary accumulation in renal parenchyma could also be caused by metallothionein upregulation in the renal tissue.

The study has limitations. The PET/CT method follows distribution of ^{64}Cu, and we assume it behaves like non-ceruloplasmin-bound copper because the naturally occurring isotopes are ^{63}Cu and ^{65}Cu and the tracer dose of ^{64}Cu was less than 0.1% of non-ceruloplasmin-bound copper in plasma. At the same time, copper may be distributed to different compartments, some of which exchange so slowly with the cytosol that we cannot detect them using the current method. Thus, in a ^{67}Cu study, the hepatic turnover of cold copper in WD rats was estimated to be as long as 1,800 days.[55] Also, we note that the methodology of the study is unable to measure the steady state concentrations of non-ceruloplasmin-bound cold copper in different tissues. However, we aimed to study the initial distribution within the 90-minute time frame, and this should not be affected by distribution into very slow compartments. Formation of ^{64}Cu ceruloplasmin is a potential bias in the kinetic analysis, but not likely to affect our findings, since earlier studies suggest that only minute amounts would be present within the 90-minute time frame used for kinetic analysis.[29] The sample size was the maximum achievable, but we cannot exclude that a larger sample would detect more group differences, however, the study was able to detect important differences between groups. We measured radioactivity in certain areas of the tissue of interest and used an estimated or standard size of the organ. These sizes may not be appropriate for all individuals and thus caused uncertainties in the estimated %ID but likely not to the extent that could affect our main conclusions. Because we did not have dynamic data (0-90 min after injection) from the brain, we estimated *K* based on the net uptake of ^{64}Cu in the brain at the 90-minute time point. Still, the very low activity of ^{64}Cu in the brain at the 90-minute time point supports our conclusion of extremely slow exchange between the blood and brain.

Our study has at least two important findings: first, temporary distribution into extrahepatic organs, especially muscles, may in the short term protect more sensitive organs, like the brain, from the effects of oscillations in the bioavailable non-ceruloplasmin-bound copper fraction – a hitherto overlooked function of muscles in copper metabolism. The large volume of these tissues led to

their notable ability to store copper in the short term and adjust the copper equilibrium between blood, muscle, and adipose tissue, which could offer therapeutic benefits in specific cases, such as acute liver failure in Wilson disease. Second, the brain takes up non-ceruloplasmin-bound copper at a rate that is 2-3-fold lower than for any other organ, emphasizing that brain copper is highly regulated, and that this regulation could be a separate treatment target for future developments.

Abbreviations

%ID, percentage of injected dose; ^{64}Cu, 64-copper or $^{64}CuCl_2$; CON, healthy controls; CTR1, copper transporter 1; HZ, parents, children, or heterozygote siblings to WDP; MBq, megabecquerel; WD, Wilson disease; WDP, patients with Wilson disease; VOI, volume of interest.

Financial support

This work was supported by a grant from The Memorial Foundation of Manufacturer Vilhelm Pedersen and Wife. The foundation played no role in the planning of the study.

Conflict of interest

The authors declare no conflicts of interest that pertain to this work.

Please refer to the accompanying ICMJE disclosure forms for further details.

Authors' contributions

DEM, MHV, PO, DB and TDS conceptualized the study. HV, PO and TDS acquired funding. KHV, DB and TDS investigated and administered the project. DEM, FTK, KSR and PO performed data analysis. MHV, OLM and TDS validated the data analysis and assisted in interpretation and visualization of the data. DEM and PO wrote the original manuscript. All authors reviewed and edited the final manuscript.

Data availability statement

Datasets are available from the corresponding author upon reasonable request.

Acknowledgements

The authors would like to thank the patients, relatives and controls who volunteered for this study – this study would not have been possible without them. Also thank you to the PET personnel for competent assistance with the scans.

Supplementary data

Supplementary data to this article can be found online at https://doi.org/10.1016/j.jhepr.2023.100916.

References

Author names in bold designate shared co-first authorship

[1] Bull PC, Thomas GR, Rommens JM, Forbes JR, Cox DW. The Wilson disease gene is a putative copper transporting P–type ATPase similar to the Menkes gene. Nat Genet 1993;5:327–337.
[2] Bartee MY, Lutsenko S. Hepatic copper-transporting ATPase ATP7B: function and inactivation at the molecular and cellular level. Biometals 2007;20:627.
[3] Cousins RJ. Absorption, transport, and hepatic metabolism of copper and zinc: special reference to metallothionein and ceruloplasmin. Physiol Rev 1985;65:238–309.
[4] Ala A, Walker AP, Ashkan K, Dooley JS, Schilsky ML. Wilson's disease. The Lancet 2007;369:397–408.
[5] European association for the study of the liver. EASL clinical practice guidelines: wilson's disease. J Hepatol 2012;56:671–685.
[6] Scheinberg IH, Sternlieb I. Wilson's disease. Philadelphia: Saunders; 1984.
[7] Walshe JM. Monitoring copper in Wilson's disease. Adv Clin Chem 2010;50:151–163.
[8] Schilsky ML, Czlonkowska A, Zuin M, Cassiman D, Twardowschy C, Poujois A, et al. Trientine tetrahydrochloride versus penicillamine for maintenance therapy in Wilson disease (CHELATE): a randomised, open-label, non-inferiority, phase 3 trial. Lancet Gastroenterol Hepatol 2022;7:1092–1102.
[9] Schilsky ML, Roberts EA, Bronstein JM, Dhawan A, Hamilton JP, Rivard AM, et al. A multidisciplinary approach to the diagnosis and management of Wilson disease: 2022 practice guidance on Wilson disease from the American Association for the Study of Liver Diseases. Hepatology Dec 7 2022. https://doi.org/10.1002/hep.32801.
[10] Ott P, Ala A, Askari FK, Czlonkowska A, Hilgers R-D, Poujois, et al. Designing clinical trials in wilson's disease. Hepatology 2021;74:3460–3471.
[11] Poujois A, Trocello J-M, Djebrani-Oussedik N, Poupon J, Collet C, Girardot-Tinant N, et al. Exchangeable copper: a reflection of the neurological severity in Wilson's disease. Eur J Neurol 2017;24:154–160.
[12] Markossian KA, Kurganov BI. Copper chaperones, intracellular copper trafficking proteins. Function, Structure, Mechanism Action 2003;68:11.
[13] Arredondo M, Núñez MT. Iron and copper metabolism. Mol Aspects Med 2005;26:313–327.
[14] Lutsenko S. Human copper homeostasis: a network of interconnected pathways. Curr Opin Chem Biol 2010;14:211–217.
[15] Sandahl TD, Gormsen LC, Kjærgaard K, Vendelbo MH, Munk DE, Munk OL, et al. The pathophysiology of Wilson's disease visualized: a human 64Cu PET study. Hepatology 2021;75:1461–1470.
[16] Nazer H, Ede RJ, Mowat AP, Williams R. Wilson's disease: clinical presentation and use of prognostic index. Gut 1986;27:1377–1381.
[17] Dhawan A, Taylor RM, Cheeseman P, De Silva P, Katsiyiannakis L, Mieli-Vergani G. Wilson's disease in children: 37-Year experience and revised King's score for liver transplantation. Liver Transplant 2005;11:441–448.
[18] Basic anatomical and physiological data for use in radiological protection: reference values. A report of age- and gender-related differences in the anatomical and physiological characteristics of reference individuals. ICRP Publication 89. Ann ICRP 2002;32:5–265.
[19] Johnson TN, Tucker GT, Tanner MS, Rostami-Hodjegan A. Changes in liver volume from birth to adulthood: a meta-analysis. Liver Transplant 2005;11:1481–1493.
[20] Pomposelli JJ, Tongyoo A, Wald C, Pomfret EA. Variability of standard liver volume estimation versus software-assisted total liver volume measurement. Liver Transplant 2012;18:1083–1092.
[21] Segal SS, White TP, Faulkner JA. Architecture, composition, and contractile properties of rat soleus muscle grafts. Am J Physiol 1986;250:C474–C479.
[22] Janssen I, Heymsfield SB, Wang ZM, Ross R. Skeletal muscle mass and distribution in 468 men and women aged 18–88 yr. J Appl Physiol 2000;89:81–88.
[23] Deurenberg P, Weststrate JA, Seidell JC. Body mass index as a measure of body fatness: age- and sex-specific prediction formulas. Br J Nutr 1991;65:105–114.
[24] Ishizu K, Yonekura Y. Clarification of a fractional uptake concept—reply. J Nucl Med 1995;36. 712-712.
[25] Neuroimaging, Part I. Newnes; 2016.
[26] Członkowska A, Rodo M, Wierzchowska-Ciok A, Smolinski L, Litwin T. Accuracy of the radioactive copper incorporation test in the diagnosis of Wilson disease. Liver Int 2018;38:1860–1866.
[27] Cox DW, Fraser FC, Sass-Kortsak A. A genetic study of Wilson's disease: evidence for heterogeneity. Am J Hum Genet 1972;24:646–666.
[28] Tauxe WN, Goldstein NP, Randall RV, Gross JB. Radiocopper studies in patients with Wilson's disease and their relatives. Am J Med 1966;41:375–380.
[29] Owen CA. Metabolism of radiocopper (Cu64) in the rat. Am J Physiol 1965;209:900–904.
[30] Owen CA. Absorption and excretion of Cu64-labeled copper by the rat. Am J Physiol 1964;207:1203–1206.
[31] Dunn MA, Green MH, Leach RM. Kinetics of copper metabolism in rats: a compartmental model. Am J Physiol 1991;261:E115–E125.

[32] Peng F, Lutsenko S, Sun X, Muzik O. Positron emission tomography of copper metabolism in the Atp7b-/- knock-out mouse model of Wilson's disease. Mol Imaging Biol 2012;14:70–78.
[33] Weiss KC, Linder MC. Copper transport in rats involving a new plasma protein. Am J Physiol 1985;249:E77–E88.
[34] Abdelsaid K, Sudhahar V, Harris RA, Das A, Youn SW, Liu Y, et al. Exercise improves angiogenic function of circulating exosomes in type 2 diabetes: role of exosomal SOD3. FASEB J 2022;36:e22177.
[35] Prohaska JR. Role of copper transporters in copper homeostasis. Am J Clin Nutr 2008;88:826S–829S.
[36] **Ralle M**, **Huster D**, Vogt S, Schirrmeister D, Burkhead JL, Capps TR, et al. Wilson Disease at a Single Cell Level: intracellular copper trafficking activates compartment-specific responses in hepatocytes. J Biol Chem 2010;285:30875–30883.
[37] Molloy SA, Kaplan JH. Copper-dependent recycling of hCTR1, the human high affinity copper transporter. J Biol Chem 2009;284:29704–29713.
[38] Clifford RJ, Maryon EB, Kaplan JH. Dynamic internalization and recycling of a metal ion transporter: Cu homeostasis and CTR1, the human Cu+ uptake system. J Cell Sci 2016;129:1711–1721.
[39] Evering WE, Haywood S, Bremner I, Wood AM, Trafford J. The protective role of metallothionein in copper-overload: II. Transport and excretion of immunoreactive MT-1 in blood, bile and urine of copper-loaded rats. Chem Biol Interact 1991;78:297–305.
[40] Scheiber IF, Mercer JFB, Dringen R. Metabolism and functions of copper in brain. Prog Neurobiol 2014;116:33–57.
[41] Weisner B, Hartard C, Dieu C. CSF copper concentration: a new parameter for diagnosis and monitoring therapy of Wilson's disease with cerebral manifestation. J Neurol Sci 1987;79:229–237.
[42] Oldendorf WH, Kitano M. Increased brain radiocopper uptake in wilson's disease. Arch Neurol 1965;13:533–540.
[43] Choi B-S, Zheng W. Copper transport to the brain by the blood-brain barrier and blood-CSF barrier. Brain Res 2009;1248:14–21.
[44] Telianidis J, Hung YH, Materia S, Fontaine SL. Role of the P-Type ATPases, ATP7A and ATP7B in brain copper homeostasis. Front Aging Neurosci 2013;5:44.
[45] Dusek P, Litwin T, Członkowska A. Neurologic impairment in Wilson disease. Ann Translational Med 2019;7. S64-S64.
[46] Kuwert T, Hefter H, Scholz D, Milz M, Weiss P, Arendt G, et al. Regional cerebral glucose consumption measured by positron emission tomography in patients with Wilson's disease. Eur J Nucl Med 1992;19:96–101.
[47] De Volder A, Sindic CJ, Goffinet AM. Effect of D-penicillamine treatment on brain metabolism in Wilson's disease: a case study. J Neurol Neurosurg Psychiatry 1988;51:947–949.
[48] Cordato DJ, Fulham MJ, Yiannikas C. Pretreatment and posttreatment positron emission tomographic scan imaging in a 20-year-old patient with Wilson's disease. Mov Disord 1998;13:162–166.
[49] Oertel WH, Tatsch K, Schwarz J, Kraft E, Trenkwalder C, Scherer J, et al. Decrease of D2 receptors indicated by 123I-iodobenzamide single-photon emission computed tomography relates to neurological deficit in treated Wilson's disease. Ann Neurol 1992;32:743–748.
[50] Schlaug G, Hefter H, Nebeling B, Engelbrecht V, Weiss P, Stöcklin G, et al. Dopamine D2 receptor binding and cerebral glucose metabolism recover after D-penicillamine-therapy in Wilson's disease. J Neurol 1994;241:577–584.
[51] Jeon B, Kim JM, Jeong JM, Kim KM, Chang YS, Lee DS, et al. Dopamine transporter imaging with [123I]-beta-CIT demonstrates presynaptic nigrostriatal dopaminergic damage in Wilson's disease. J Neurol Neurosurg Psychiatry 1998;65:60–64.
[52] Gray LW, Peng F, Molloy SA, Pendyala VS, Muchenditsi A, Muzik O, et al. Urinary copper elevation in a mouse model of Wilson's disease is a regulated process to specifically decrease the hepatic copper load. PLoS One 2012;7:e38327.
[53] Peng F, Lutsenko S, Sun X, Muzik O. Imaging copper metabolism imbalance in Atp7b (-/-) knockout mouse model of Wilson's disease with PET-CT and orally administered 64CuCl2. Mol Imaging Biol 2012;14:600–607.
[54] **Linz R**, **Barnes NL**, Zimnicka AM, Kaplan JH, Eipper B, Lutsenko S. Intracellular targeting of copper-transporting ATPase ATP7A in a normal and Atp7b−/− kidney. Am J Physiol 2008;294:F53–F61.
[55] Gibbs K, Walshe JM. Studies with radioactive copper (64 Cu and 67 Cu); the incorporation of radioactive copper into caeruloplasmin in Wilson's disease and in primary biliary cirrhosis. Clin Sci 1971;41:189–202.